# Journal of Materials Chemistry C

## Recent advances in materials and device technologies for soft active matrix electronics

SCHOLARONE™
Manuscripts

# Recent advances in materials and device technologies for soft active matrix electronics

Hyunseok Shim[a], Kyoseung Sim[b,c], Faheem Ershad[d], Seonmin Jang[a], and Cunjiang Yu[*,a,b,d,e]

[a]Materials Science and Engineering Program, University of Houston, Houston, TX, 77204, USA

[b]Department of Mechanical Engineering, University of Houston, Houston, TX, 77204 USA

[c]Department of Chemistry, Ulsan National Institute of Science and Technology (UNIST), Ulsan 44919, Republic of Korea

[d]Department of Biomedical Engineering, University of Houston, Houston, TX, 77204, USA

[e]Department of Electrical and Computer Engineering, Texas Center for Superconductivity, University of Houston, Houston, TX, 77204, USA

E-mail: cyu15@uh.edu

Keywords: active matrix, flexible electronics, stretchable electronics, transistors

**Biographies and Pictures:**



Hyunseok Shim received his BS in Electronics and Radio Engineering in 2011 from the Kyung Hee University, and a MS in Physical Chemistry in 2014 from the Konkuk University, Korea. He was a researcher in Daegu Gyeongbuk Institute of Science and Technology (South Korea) from 2014 to 2017. He is currently pursuing Ph.D. degree in Materials Science and Engineering at University of Houston. His current research focuses on soft electronics.



Dr. Cunjiang Yu is the Bill D. Cook Associate Professor in the Department of Mechanical Engineering at University of Houston. He received his Ph.D. degree in Mechanical Engineering from Arizona State University in 2010. He was a post-doctoral fellow in the Department of Materials Science and Engineering at University of Illinois at Urbana-Champaign between 2010 and 2013. He is a recipient of NSF CAREER Award, ONR Young Investigator Award, MIT Technology Review Top Innovator, AVS Young Investigator Award, etc. His current research focuses on soft electronics and bioelectronics.

**Abstract:**

Multiplexed active matrix addressing is critical to extract and process signals from a large number of channels. Recently, the soft active matrix has attracted a great deal of attention due to its potential for a variety of applications such as electronic skins, sensors, and bioelectronics. To realize their use in these various applications, flexible and stretchable formats of the active matrix technologies have emerged. In this review, a variety of reports on the soft active matrix are presented and discussed. The technologies of electronic devices implemented in the modern active matrix are introduced. Strategies to achieve flexible and stretchable active matrix technologies, their advantages and disadvantages, and their applications are briefly described. The review closes with a summary, the associated challenges, and future directions on the development of soft active matrix electronics.

# 1. Introduction

Along with the display industry, matrix addressing with both passive and active matrix technologies have been steadily developed. Early on, passive matrix technologies could be found in products with liquid crystal displays (LCDs), such as digital clocks and calculators[1]. In a passive matrix, each pixel in a grid is defined by the intersecting electrode of the top and bottom substrates, and a voltage waveform is applied to each pixel to turn the pixels on. Typically, this requires controlling voltages at the electrical junctions of the grid to turn on a single pixel, making the response times of the passive matrix slow, and thus, unable to correctly show rapid motions on a display. Active matrix addressing overcame that limitation through the attachment of active devices, which serve as switches, to each pixel. Driving the active devices allows for individual control of pixels[2]. The concept of active matrix addressing was first introduced into the literature in 1975[3]. Generally, diodes or transistors serve as the two-terminal or three-terminal based active devices, respectively[4-7]. The advancements in active matrix addressing have allowed the technology utilization to increase beyond the display industry into various other medical applications such as electronic skins (e-skins), sensors, and bioelectronics. However, these applications require that the active matrix technologies be made in compliant formats, that is soft and stretchable, in order to adequately conform to the soft, curvilinear, and dynamic target surfaces of the human body.

Due to the immense need for wearable and implantable electronic devices in healthcare, soft electronics, which have been shown to produce conformal contact, accurate measurements, and enhanced biocompatibility, have been extensively investigated[8-11]. Examples of soft electronics with active matrix technologies are shown in **Figure 1**. The devices are stretchable (**Figure 1** (a)) and make conformal contact with the moving organs of a mammal (**Figure 1** (b)) and a human palm (**Figure 1** (c)) to accurately sense the signals[12-14].

Approaches to develop conventionally rigid electronics into flexible and stretchable

formats involve reducing the thickness of the electronics and arranging the materials into structures that can accommodate strain. To make the deformable counterparts to rigid electronics, strategies of structural engineering of rigid materials, such as pre-straining, in-plane serpentine, and kirigami has been widely adopted[15-17]. Furthermore, employing intrinsically stretchable or rubbery materials has been an alternative strategy to structural engineering to achieve device stretchability. For instance, electronics in both flexible and stretchable formats even based on one type of material, such as poly(3,4-ethylenedioxythiophene)-poly(styrene sulfonate) (PEDOT:PSS), have been developed using the aforementioned strategies[18-27]. Alongside the need for wearable and implantable devices is the requirement for higher spatial resolution to detect signals and resolve features for improved diagnosis and treatment of health conditions[28]. A higher density and number of electrodes can more effectively map tissues/organs of the human body and ultimately improve healthcare decisions and outcomes[29]. For these reasons, there has been an emphasis on developing active matrix technologies using soft electronics.

This review presents an overview of the recent progress in flexible and stretchable active matrix technologies and discusses their material/device constructions, performances in the presence of mechanical deformation, and various applications. Specifically, the first section of this review highlights the advantages/disadvantages of the active matrix, emphasizes the importance of transistor technologies, and explains the active matrix operation principles. In the following section, we introduce flexible active matrix electronics that have been constructed based on arrayed inorganic and organic transistors. Stretchable active matrix electronics developed with different strategies to achieve stretchability are discussed in the third section. We conclude with a summary and remarks on the associated challenges in soft active matrix electronics and possible future directions.

## 2. Active matrix

Matrix addressing has been the immediate successor to direct addressing. The schematic circuit diagram in **Figure 2** shows the difference between the two types[30-32]. Direct addressing is a method of transmitting signals by connecting all the individual output terminals of the driver integrated circuit (IC) and to each pixel, as shown in **Figure 2** (a). **Figure 2** (b) presents that matrix addressing, including both active and passive matrix addressing, is a method of transmitting signals to a plurality of pixels using one set of wiring. In terms of the connection complexity, the number of wires required for direct addressing in an m × n pixel array is m × n. However, in matrix addressing, only m wires are needed when the data lines are formed vertically. As a result, matrix addressing has the advantage of significantly reducing the number of wires compared to direct addressing, which is crucial for minimizing the overall size of the device and simultaneously allows for higher density and higher resolution arrays. Furthermore, it is important to consider the differences between the modes of matrix addressing, namely, passive and active matrix addressing.

In the case of the passive matrix addressing, the signal voltage can affect neighboring pixels, otherwise known as crosstalk. Therefore, as the number of electrodes increases, the contrast sharply decreases and the image quality deteriorates. On the other hand, in the case of active matrix addressing, crosstalk between the pixels can be eliminated since the pixels can be adjusted by using the active devices. This method guarantees excellent image quality and displays with high aspect ratios, making the active matrix suitable for high-resolution displays. Therefore, active matrix addressing is a more advanced method compared to passive matrix addressing. The slight disadvantage is that the cost to produce this technology is increased because an active device is used for each pixel, but the tradeoff has been shown to be more beneficial[33].

**Figure 3** shows the typical transistor array for active matrix addressing. Active matrix

addressing relies on the stable performance of each pixel. Typically, each pixel consists of transistors, which are the basic building blocks of electronic circuitry. By ensuring uniform characteristics of the transistors and rationally arranging them, a reliable active matrix can be made. The operation principle of an m × n active matrix, particularly in the context of displays, is described in the following. When the scan line is selected sequentially, it emits light continuously according to the signal of the data line until the next frame is inputted. For example, if a circuit operates with passive matrix addressing, n pixels are turned on when the first gate line is activated. After those n pixels turned off, the second gate line will operate[34]. However, if the circuit is operated with active matrix addressing, selected pixels will be turned on when the first gate line is activated, and the second gate line will be activated before pixels from the first line are turned off. This occurs because capacitors are connected to the pixels, allowing for stored information to be kept until the end of one frame so that the image can be shown correctly[6]. Again, compared to direct addressing, only m wires are needed when the data lines are formed vertically, as mentioned above. However, in order to perform the ON/OFF operation of the switches, wires for controlling the switches are required. This wire is formed in a direction intersecting the data wiring and simultaneously controls several switches connected to the wire. Therefore, the number of wires required for driving the active matrix is the sum of m data lines and n gate lines, which reduces the number of wires that would be required by direct addressing. It is important to note that gate and data lines are sometimes referred to as word and bit lines, respectively. In addition, active matrix addressing is suitable for various applications because the active matrix can be driven at a low voltage and the driving circuit is inside the matrix, allowing for miniaturization. In the following sections, we have detailed the flexible and stretchable active matrix technologies and their applications. Specifically, the associated materials and their applications are summarized in **Table 1**.

### 3. Flexible active matrix

### 3.1. Flexible active matrix based on inorganic electronics

Recently, active matrix electronics have been developed into flexible formats so that they can deform or conformally lay on the surfaces of organs and biological tissues. Flexible active matrix constructed from electronic devices, including diodes and transistors, based on inorganic semiconductor materials has offered advantages such as higher carrier mobility, lower operation voltage and improved flexibility, as discussed in the following studies[5, 35-53]. Multiple approaches to achieve flexible active matrix devices have been reported, such as transfer printing inorganic materials (e.g. ultra-thin films and nanowires) on flexible substrates have been achieved through various process schemes[54-59].

Yu *et al*. developed a flexible multiplexed adaptive optoelectronic camouflage skin based on ultrathin silicon (Si) diode active matrix[5]. The camouflage skin pursued a multilayer configuration with two layers of active matrix electronics: one layer for active matrix based light sensing and another layer for active matrix based, thermally induced color modulation. **Figure 4** (a) presents a schematic illustration of a $16 \times 16$ array of interconnected unit cells in a full, adaptive camouflage skin, where the two layers of the Si diode based active matrix are employed for light sensing and for thermal actuation. **Figure 4** (b) is the schematic illustration of the sensing part in this system. Distributed active matrix sensing of background patterns was achieved through arrays of thin Si photodiodes. The photodiodes were positioned at the notches to allow exposure to the light incident on the system (from above or below) and the multiplexing blocking diode incorporated an opaque coating to eliminate its sensitivity to light. A circuit diagram for the sensing part is shown in **Figure 4** (c). The voltage pattern that was obtained from light sensing was used to trigger the thermal actuator pixels accordingly, which is schematically illustrated in **Figure 4** (d). Specifically, an array of ultrathin Si diodes provided local Joule heating, also with the capability of multiplexed addressing automatically. The active

matrix Si diode based thermal actuator induced changes in the thermochromic materials' color in a reflective manner. The circuit diagram for the flexible, diode based active matrix thermal actuator is presented in **Figure 4** (e). The actuation and sensing layers showed excellent flexibility due to their thin construction. No delamination occurred when the device was bent to a radius of 2 mm. The maximum strain in silicon depending on the bending radius is shown in **Figure 4** (f). An image of the bent camouflage system is illustrated in **Figure 4** (g).

Takei *et al.* investigated a flexible active matrix based artificial skin using Ge/Si nanowires (NW) as the active material on a polyimide substrate due to its advantages such as low operation voltage, superb mechanical robustness, and reliability[37]. Ge/Si core/shell NW parallel arrays were transferred to lithographically predefined active regions by a contact-printing method, as described in detail in elsewhere[58, 60]. Afterward, a Ni thin film was deposited to serve as the source and drain electrodes. A schematic exploded view and optical image of the flexible active matrix based e-skin is presented in **Figure 5** (a), which shows outstanding mechanical flexibility of all integrated components. A single pixel of the active matrix employed a Ge/Si NW based field effect transistor (FET) that was connected to pressure-sensitive rubber (PSR) in a $19 \times 18$ array as shown in **Figure 5** (b). The gate and drain bias of Ge/Si NW FETs were used as the word and bit lines of the active matrix, respectively. A mapping of the applied pressure was obtained by measuring the conductance of each pixel in the active matrix. In order to confirm the performance of the flexible active matrix based e-skin, a 'C' shaped PDMS mold was placed on top of e-skin. **Figure 5** (c) shows both the design layout of the active matrix and the corresponding mapping results. Despite a few defective pixels, the active matrix could clearly map applied pressures.

A flexible inorganic transistor based active matrix can be used not only for e-skin, but also as a tool for acquiring biological signals. Fang *et al.* reported a capacitively coupled silicon array using a silicon nanomembrane based transistor for long-term cardiac electrophysiology[46].

Silicon nanomembranes enable high performance and are compatible with capacitively coupled systems which are formed by depositing an ultrathin thermal $SiO_2$ layer on top of a Si NMOS array. **Figure 5** (d) shows an exploded view of a completed capacitively coupled flexible sensing system with an active matrix. The matrix consisted of $18 \times 22$ capacitive sensors. The thermally grown $SiO_2$ layer functioned as the dielectric for capacitive coupling between biological tissue and the semiconducting channels, as well as a barrier layer that hinders the penetration of bio-fluids. The inset of **Figure 5** (d) shows a photograph of the capacitively coupled sensor array, which shows good flexibility. A circuit diagram for the individual sensor is shown in **Figure 5** (e). Each sensor consisted of an amplifier and a multiplexer with a capacitive input pad. The signal obtained through the capacitive input pad was transmitted through an amplifier and was controlled by a multiplexer. A circuit diagram of a common drain amplifier (source follower) is presented in **Figure 5** (f). This circuit provided an optimal voltage gain of 1 as a result of the large capacitive coupling. The response to the sine wave input before and after the bending and soaking experiment is shown in **Figure 5** (g). The characterization results from those experimental conditions demonstrated that the device is suitable for the conditions of the *in vivo* cardiac environment. **Figure 5** (h) shows electrophysiological signal mapping from a rabbit heart during the sinus rhythm. The results show that the proposed system can map the electrical signals of the heart with high resolution while maintaining conformal contact with the heart as shown in the inset of **Figure 5** (h).

### 3.2. Flexible active matrix based on organic electronics

An inorganic material such as Si must be made thin to ensure mechanical flexibility, which typically involves dedicated microfabrication processes[61-64]. However, organic materials which have lower moduli are well suited to be used for flexible electronics. In addition, the fabrication can be based on relatively simple and low-cost processes as compared to those

utilized with inorganic materials[65-67]. Many studies have been also reported on the flexible

organic transistor based active matrix[4, 68-91]. However, the literature has been mainly limited to

displays and there are few reports on other applications[92-95]. Someya *et al.* proposed an artificial

skin using an organic semiconductor based flexible pressure sensor matrix in 2004[68]. In this

work, a flexible active matrix was for the first time developed for a pressure sensor array, which

shows many advantages such as low power consumption and less crosstalk. Since then, the

flexible organic semiconductor active matrix has been actively developed for a variety of

applications such as e-skin, sensors, actuators, and memory[71, 74, 80, 86-91].

Ren. *et al.* reported a flexible active matrix for temperature mapping using a

Dinaphthothienothiophene (DNTT) based organic transistor[87]. A thin ( ~12 μm) poly(ethylene

naphthalate) (PEN) film was used for the substrate which offers high flexibility and bending

stability. **Figure** 6 (a) shows a schematic illustration of the $16 \times 16$ array, single pixel, and

circuit diagram. The pentacene/silver nanoparticles (NPs) based thermistor was directly

connected to the drain electrode of an organic transistor for sensing the temperature. Because

the resistance of the thermistor varies depending on temperature, differences in the drain

current could be detected as the temperature changed. To demonstrate its potential for use in

biomedical applications, the active matrix based temperature sensor array was placed on a

human subject's forehead as shown in **Figure 6** (b). An advantage of the PEN substrate was

that Vaseline could be added for better contact between the flexible active matrix and the skin.

**Figure 6** (c) presents the measured temperature distribution after placing the flexible active

matrix on the forehead which suggests that the device can be used for human body temperature

sensing applications.

Similarly, Sekitani *et al.* demonstrated the flexible organic transistor based active

matrix for *in vivo* biological signal mapping (**Figure** 6 (d))[96]. To capture weak signals, a small

signal amplifier was constructed using four DNTT-based organic transistors, a resistor, and a

capacitor connected to the sensing part of the active matrix. **Figure 6** (e) shows a circuit diagram of the flexible active matrix amplifier array. The amplifiers were connected to the source electrodes of the organic transistor. The active matrix was adhered to skin using conductive gel. The small signals obtained through the gel were amplified by the amplifier. Each transistor was controlled by the word line, which enabled the selectively amplified signal to be received from the bit line. **Figure 6** (f, left) shows the photograph of the organic pseudo-CMOS inverter that was used as the amplifier. To operate the organic pseudo-CMOS inverter, separate voltages including $V_{DD}$, $V_{SS}$, and GND were applied to a circuit of the inverter. The voltage transfer curve (VTC) and gain of the organic pseudo-CMOS inverter are shown in **Figure 6** (f, right), which shows no obvious degradation before and after being used to contact a rat heart. The obtained gain from the characterization allows for predicting the degree of amplification of the small biological signal. **Figure 6** (g) presents clear amplification of the signal attained from the *in vivo* rat heart.

## 4. Stretchable active matrix

### 4.1. Stretchable active matrix based on stretchable interconnects

Although the flexible active matrix has been extensively reported, the stretchable active matrix has been of great interest as it can accommodate large strain when adhered to curvy, irregular surfaces and their associated motions[12, 14, 97-103]. Gray *et al.* proposed the island/bridge interconnection approach for inorganic materials based stretchable electronics, making it possible to construct an active matrix in stretchable formats and enabling a variety of applications[104]. Choi *et al.* reported a Si transistor based stretchable active matrix for a display based on a similar approach [97]. **Figure 7** (a) schematically shows a micro-light emitting diode (μLED) directly connected to a Si transistor in a typical pixel based display. An intrinsically non-stretchable Au film was patterned in a serpentine shape to ensure stretchability

and was utilized as the interconnects between the rigid island pixels and circuitry in the active matrix. The circuit diagram of the active matrix is shown in **Figure 7** (b). As discussed earlier in **Figure 2**, the circuit structure is a typical transistor array for multiplexed active matrix addressing. When the gate signal was sequentially selected, the μLED emitted light according to a data signal. **Figure 7** (c) shows the dynamic operation of the active matrix on a polydimethylsiloxane (PDMS) substrate. The active matrix display was used to depict the word "YONSEI" by changing the gate and data lines in real time. The active matrix display functioned normally with no cracks or line disconnection under a mechanical strain of 40% as shown in **Figure 7** (d). The shape of the letter "N" remained discernable under mechanical strain and the light emission was uniform (no degradation) because of the strain accommodation by the mechanically deformed serpentine shaped stretchable interconnects (**Figure 7** (e)).

Architectural engineering of stretchable interconnects involves sophisticated fabrication processes and low integration density, which limits the applications of electronics developed using those strategies. An alternative strategy for the stretchable active matrix involves using intrinsically stretchable interconnects with rigid islands based active electronics[12, 98-102].

Sekitani *et al.* reported a stretchable active matrix using a single wall carbon nanotube (SWNT) elastic conductor and paste based stretchable interconnects[98]. Pentacene was used as the organic semiconductor for transistors fabricated on a polyimide substrate, which is not stretchable, as shown in **Figure 8** (a). Taking advantage of the SWNT elastic conductor and paste, 19 × 37 organic transistors based stretchable active matrix with stretchable SWNT interconnection was fabricated. Each transistor was placed on silicone rubber and the elastic conductor and paste were implemented for the interconnects, word lines, and bit lines. A schematic illustration of the stretchable active matrix is shown in **Figure 8** (b). The active

matrix shows no cracks or damages at 70% biaxial stretching, as pictured in **Figure 8** (c). In addition, no significant degradation of the device performance was observed (**Figure 8** (d)) which implies that the active matrix using rigid islands and intrinsically stretchable interconnection is mechanically and electrically stable under biaxial strain.

Liquid metal is another potential promising candidate for interconnects of stretchable electronics because it remains conductive even under a mechanical strain of ~ 300%[105, 106]. Park *et al.* reported a stretchable active matrix using liquid metal for interconnects and IGZO as the semiconductor for the rigid island transistor on a polyimide substrate[101]. Here, the liquid metal was patterned by a photolithography-based technique compatible with conventional flexible circuit technology to form the interconnects. **Figure 8** (e) shows the optical microscope image and schematic cross-sectional view of the IGZO based transistor. To demonstrate the benefit of using liquid metal, a 4 × 4 active matrix array based on IGZO transistors was fabricated and mechanically and electrically characterized. The circuit diagram of the active matrix is shown in **Figure 8** (f, left). Liquid metal was used for the interconnects, including the bit, data, and GND lines. The combination of rigid transistors and liquid metal interconnects functioned stably under a mechanical deformation of 40% as shown in **Figure 8** (f, right). In addition, the transfer characteristics of the oxide transistor showed no change under a mechanical strain of 40%, as shown in **Figure 8** (g).

## 4.2. Stretchable active matrix all based on intrinsically stretchable, rubbery electronics

The approach of using rigid islands and stretchable interconnects to create the stretchable active matrix is promising, but some disadvantages remain. Since stretchable interconnects are required between transistor units, there is a trade-off between device density and stretchability. Also, the manufacturing process is complicated and not compatible with fully solution processable fabrication methods. Recently, another strategy for implementing a

stretchable active matrix has been enabled by the use of all rubber-like intrinsically stretchable materials (e.g. rubbery semiconductor, conductor, and gate dielectric) for fabricating stretchable transistors[14, 103, 107-109]. This approach has excellent advantages such as high mechanical stability, simple device structure for the active matrix, and easy fabrication in a solution processable manner[14, 103]. Thus, efforts have been made to develop the intrinsically stretchable active matrix based on such stretchable transistors.

Wang *et al.* produced a tactile sensing skin based on an intrinsically stretchable active matrix. The transistors in the $10 \times 10$ active matrix were constructed using all stretchable materials, including a polymeric semiconductor/elastomer composite (29-DPP-SVS/polystyrene-block-poly(ethylene-ran-butylene)-block-polystyrene (SEBS)), SEBS, and CNT as the stretchable semiconductor, gate dielectric, and conductor, respectively. The transistors showed stable operation under a mechanical strain of 100%[14]. The intrinsically stretchable active matrix for tactile sensing was constructed by connecting the drain electrode of the transistor to the resistive tactile sensor for each pixel. In addition, a scan line and a data line were connected to the gate electrode and the source electrode, respectively, as shown in **Figure 9** (a). When the resistance of the tactile sensor was altered by physical touching, a voltage was applied to the drain electrode and current flowed accordingly, depending on the gate voltage. One of the primary advantages of the intrinsically stretchable active matrix is that a separate structural design is not required to fabricate a stretchable active matrix because all the materials that compose the active matrix are intrinsically stretchable. **Figure 9** (b) shows the image of the stretchable active matrix and the inset shows the transfer characteristics of a single transistor. The high stretchability of the active matrix allows it to be attached conformally to the human palm. **Figure 9** (c) shows an optical image of an artificial ladybug that was placed on the tactile sensing active matrix and the corresponding tactile mapping, which indicates the detected pressure from the six legs of the ladybug. The results showed the

feasibility of a stretchable active matrix as a backplane for high-resolution tactile sensing.

Sim *et al.* recently reported a fully rubbery active matrix for tactile sensing skin using high performance rubbery transistors based on a multi-wall carbon nanotube (CNT) doped poly(3-hexylthiophene) nanofibril (P3HT-NF)/PDMS composite as the semiconducting material[103]. **Figure 9** (d) shows the circuit diagram of a single pixel of the stretchable active matrix based tactile sensing skin, which was constructed by connecting the rubbery transistors and PSR based tactile sensors. The tactile sensors had a very low resistance under applied pressure, but without pressure, the sensors had high resistance, and thus the drain voltage could be applied to the rubbery transistor. By selectively controlling the word line, current flowed accordingly through the bit line. This current was then detected as a voltage across a resistor which was appropriately chosen. When the drain voltage of -1 V was applied to the transistor, an output of -1 V was measured once the tactile sensor was pressed. **Figure 9** (e) shows the deformed fully rubbery active matrix under mechanical stretching. In order to confirm that the proposed fully rubbery active matrix functioned as a tactile sensing skin, an arbitrarily shaped object was placed on top of the active matrix. **Figure 9** (f) shows the voltage mapping results before and after applying mechanical strain of 30% along the channel length direction and no significant difference in mapping results before and after stretching was observed.

## 5. Summary, Challenges, and Outlook

### 5.1. Summary

Multiplexed active matrix addressing has been successfully implemented for a variety of applications, however, numerous challenges still need to be overcome. For example, there are many reports on rigid and flexible active matrix technologies, but there are limited reports on stretchable active matrix technologies partially because they are more difficult to realize. Of course, the results for existing flexible active matrix demonstrate that they can serve as

16

electronic skins, sensors, and bioelectronics, but further research on stretchable active matrix technologies is urgently required to match the increasing needs in wearable, portable, stretchable and implantable electronics.

## 5.2. Challenges

Some representative challenges to develop soft active matrix technologies are as follows. For instance, even though there are a few existing reports on stretchable active matrix technologies, typically the driving voltages are fairly high[98, 101], which poses biosafety issues for biomedical applications[14, 110]. In other words, low operation voltages for stretchable active matrix technologies are needed[103, 109]. In addition, the next generation of wearable and implantable devices urgently requires high spatiotemporal resolution. Therefore, further studies on intrinsically stretchable, rubbery electronics are required to enable high spatial resolution (high density). In addition, the operation speed of the transistors also needs to increase to enable high temporal resolution. As mentioned before, the stretchable active matrix all based on intrinsically stretchable, rubbery transistors does not require a separate structural design (which requires large areas for interconnects) and thus, it can be used to implement a higher density of devices[14]. Simultaneously, issues such as poor stability and relatively low carrier mobility which are generally associated with the use of organic electronic materials need to be resolved[111, 112]. Manufacturing technologies to pattern intrinsically stretchable semiconductors, conductors, and dielectrics must be improved for precise patterning at the micro/nanoscale[113-117]. To simultaneously realize high mechanical strain tolerance and electrical performances is also essential, which requires a deep understanding of the structure-property relationships between electronic materials and their mechanical and electrical properties[118]. Furthermore, the rational integration of the soft active matrix with sensors of high sensitivity, conformability, and biocompatibility is another consideration for accurate and

precise biological signal acquisition from tissues such as the heart, muscle, and brain tissues.


### 5.3. Outlook

Although many challenges remain, future research and development in active matrix addressing technology and its applications are promising. Due to its soft mechanical attributes, the soft active matrix can be investigated and employed for further applications where a large number of signals are extracted from soft objects such as human and animal bodies, organs, tissues, and machine interfaces devices among others[13, 38, 46, 88, 96].

**Conflicts of interest**

The authors declare no competing financial interests.

**Acknowledgements**

## Notes and references

1.  L. Goodman, *IEEE Transactions on Consumer Electronics*, 1975, 247-259.
2.  W. F. Aerts, S. Verlaak and P. Heremans, *IEEE Trans. Electron Devices*, 2002, **49**, 2124-2130.
3.  T. Brody, F. C. Luo, Z. P. Szepesi and D. H. Davies, *IEEE Trans. Electron Devices*, 1975, **22**, 739-748.
4.  N. Matsuhisa, H. Sakamoto, T. Yokota, P. Zalar, A. Reuveny, S. Lee and T. Someya, *Advanced Electronic Materials*, 2016, **2**, 1600259.
5.  C. Yu, Y. Li, X. Zhang, X. Huang, V. Malyarchuk, S. Wang, Y. Shi, L. Gao, Y. Su and Y. Zhang, *Proceedings of the National Academy of Sciences*, 2014, **111**, 12998-13003.
6.  M. L. Chabinyc and A. Salleo, *Chem. Mater.*, 2004, **16**, 4509-4521.
7.  G. Gelinck, P. Heremans, K. Nomoto and T. D. Anthopoulos, *Adv. Mater.*, 2010, **22**, 3778-3798.
8.  D.-H. Kim, Y.-S. Kim, J. Amsden, B. Panilaitis, D. L. Kaplan, F. G. Omenetto, M. R. Zakin and J. A. Rogers, *Applied physics letters*, 2009, **95**, 133701.
9.  J. Reeder, M. Kaltenbrunner, T. Ware, D. Arreaga-Salas, A. Avendano-Bolivar, T. Yokota, Y. Inoue, M. Sekino, W. Voit and T. Sekitani, *Adv. Mater.*, 2014, **26**, 4967-4973.
10. K. Fukuda, Y. Takeda, Y. Yoshimura, R. Shiwaku, L. T. Tran, T. Sekine, M. Mizukami, D. Kumaki and S. Tokito, *Nat. Commun.*, 2014, **5**, 4147.
11. D. Son, J. Lee, S. Qiao, R. Ghaffari, J. Kim, J. E. Lee, C. Song, S. J. Kim, D. J. Lee and S. W. Jun, *Nat. Nanotechnol.*, 2014, **9**, 397.
12. N. Matsuhisa, M. Kaltenbrunner, T. Yokota, H. Jinno, K. Kuribara, T. Sekitani and T. Someya, *Nature communications*, 2015, **6**, 7461.
13. J. Viventi, D.-H. Kim, J. D. Moss, Y.-S. Kim, J. A. Blanco, N. Annetta, A. Hicks, J. Xiao, Y. Huang and D. J. Callans, *Science translational medicine*, 2010, **2**, 24ra22-24ra22.
14. S. Wang, J. Xu, W. Wang, G.-J. N. Wang, R. Rastak, F. Molina-Lopez, J. W. Chung, S. Niu, V. R. Feig and J. Lopez, *Nature*, 2018, **555**, 83-88.
15. X. Feng, B. D. Yang, Y. Liu, Y. Wang, C. Dagdeviren, Z. Liu, A. Carlson, J. Li, Y. Huang and J. A. Rogers, *Acs Nano*, 2011, **5**, 3326-3332.
16. C. Dagdeviren, Y. Shi, P. Joe, R. Ghaffari, G. Balooch, K. Usgaonkar, O. Gur, P. L. Tran, J. R. Crosby and M. Meyer, *Nat. Mater.*, 2015, **14**, 728.
17. M. Isobe and K. Okumura, *Scientific reports*, 2016, **6**, 24758.
18. W. Lee and T. Someya, *Chemistry of Materials*, 2019, **31**, 6347-6358.
19. X. Fan, W. Nie, H. Tsai, N. Wang, H. Huang, Y. Cheng, R. Wen, L. Ma, F. Yan and Y. Xia, *Advanced Science*, 2019, **6**, 1900813.
20. L. V. Kayser and D. J. Lipomi, *Advanced Materials*, 2019, **31**, 1806133.
21. H. Yuk, B. Lu, S. Lin, K. Qu, J. Xu, J. Luo and X. Zhao, *Nature communications*, 2020, **11**, 1-8.
22. D. J. Lipomi and Z. Bao, *Energy & Environmental Science*, 2011, **4**, 3314-3328.
23. R. Zhou, P. Li, Z. Fan, D. Du and J. Ouyang, *Journal of Materials Chemistry C*, 2017, **5**, 1544-1551.
24. M. Y. Teo, N. Kim, S. Kee, B. S. Kim, G. Kim, S. Hong, S. Jung and K. Lee, *ACS applied materials & interfaces*, 2017, **9**, 819-826.
25. W. Lee, D. Kim, N. Matsuhisa, M. Nagase, M. Sekino, G. G. Malliaras, T. Yokota and T. Someya, *Proceedings of the National Academy of Sciences*, 2017, **114**, 10554-

10559.

26.    J. H. Lee, Y. R. Jeong, G. Lee, S. W. Jin, Y. H. Lee, S. Y. Hong, H. Park, J. W. Kim, S.-S. Lee and J. S. Ha, *ACS applied materials & interfaces*, 2018, **10**, 28027-28035.

27.    K. Yamagishi, T. Nakanishi, S. Mihara, M. Azuma, S. Takeoka, K. Kanosue, T. Nagami and T. Fujie, *NPG Asia Materials*, 2019, **11**, 1-13.

28.    F. Ershad, K. Sim, A. Thukral, Y. S. Zhang and C. Yu, *APL Materials*, 2019, **7**, 031301.

29.    A. M. Taplin, A. de Pesters, P. Brunner, D. Hermes, J. C. Dalfino, M. A. Adamo, A. L. Ritaccio and G. Schalk, *Epilepsy & behavior case reports*, 2016, **5**, 46-51.

30.    P. A. Ersman, J. Kawahara and M. Berggren, *Org. Electron.*, 2013, **14**, 3371-3378.

31.    X. Zhang, P. Li, X. Zou, J. Jiang, S. H. Yuen, C. W. Tang and K. M. Lau, *IEEE Photonics Technology Letters*, 2019, **31**, 865-868.

32.    T. N. Ruckmongathan, *Addressing techniques of liquid crystal displays*, John Wiley & Sons, 2014.

33.    T. Sekitani and T. Someya, *Adv. Mater.*, 2010, **22**, 2228-2246.

34.    H. Kubota, S. Miyaguchi, S. Ishizuka, T. Wakimoto, J. Funaki, Y. Fukuda, T. Watanabe, H. Ochi, T. Sakamoto and T. Miyake, *J. Lumin.*, 2000, **87**, 56-60.

35.    J.-S. Park, T.-W. Kim, D. Stryakhilev, J.-S. Lee, S.-G. An, Y.-S. Pyo, D.-B. Lee, Y. G. Mo, D.-U. Jin and H. K. Chung, *Applied Physics Letters*, 2009, **95**, 013503.

36.    J.-S. Yoo, S.-H. Jung, Y.-C. Kim, S.-C. Byun, J.-M. Kim, N.-B. Choi, S.-Y. Yoon, C.-D. Kim, Y.-K. Hwang and I.-J. Chung, *Journal of display technology*, 2010, **6**, 565-570.

37.    K. Takei, T. Takahashi, J. C. Ho, H. Ko, A. G. Gillies, P. W. Leu, R. S. Fearing and A. Javey, *Nat. Mater.*, 2010, **9**, 821.

38.    J. Viventi, D.-H. Kim, L. Vigeland, E. S. Frechette, J. A. Blanco, Y.-S. Kim, A. E. Avrin, V. R. Tiruvadi, S.-W. Hwang and A. C. Vanleer, *Nat. Neurosci.*, 2011, **14**, 1599.

39.    T. Takahashi, K. Takei, A. G. Gillies, R. S. Fearing and A. Javey, *Nano Lett.*, 2011, **11**, 5408-5413.

40.    C. Wang, D. Hwang, Z. Yu, K. Takei, J. Park, T. Chen, B. Ma and A. Javey, *Nat. Mater.*, 2013, **12**, 899.

41.    T. Takahashi, Z. Yu, K. Chen, D. Kiriya, C. Wang, K. Takei, H. Shiraki, T. Chen, B. Ma and A. Javey, *Nano Lett.*, 2013, **13**, 5425-5430.

42.    J. T. Smith, B. O'Brien, Y.-K. Lee, E. J. Bawolek and J. B. Christen, *Journal of Display Technology*, 2014, **10**, 514-520.

43.    Q. Sun, W. Seung, B. J. Kim, S. Seo, S. W. Kim and J. H. Cho, *Adv. Mater.*, 2015, **27**, 3411-3417.

44.    C. Yeom, K. Chen, D. Kiriya, Z. Yu, G. Cho and A. Javey, *Adv. Mater.*, 2015, **27**, 1561-1566.

45.    X. Cao, C. Lau, Y. Liu, F. Wu, H. Gui, Q. Liu, Y. Ma, H. Wan, M. R. Amer and C. Zhou, *ACS nano*, 2016, **10**, 9816-9822.

46.    H. Fang, K. J. Yu, C. Gloschat, Z. Yang, E. Song, C.-H. Chiang, J. Zhao, S. M. Won, S. Xu and M. Trumpis, *Nature biomedical engineering*, 2017, **1**, 0038.

47.    J. Li, E. Song, C.-H. Chiang, K. J. Yu, J. Koo, H. Du, Y. Zhong, M. Hill, C. Wang and J. Zhang, *Proceedings of the National Academy of Sciences*, 2018, **115**, E9542-E9549.

48.    M. Choi, Y. J. Park, B. K. Sharma, S.-R. Bae, S. Y. Kim and J.-H. Ahn, *Sci. Adv.*, 2018, **4**, eaas8721.

49.    L. Nela, J. Tang, Q. Cao, G. Tulevski and S.-J. Han, *Nano Lett.*, 2018, **18**, 2054-2059.

50.   T.-Y. Zhao, D. Zhang, T.-Y. Qu, L.-L. Fang, Q.-B. Zhu, Y. Sun, T.-H. Cai, M. Chen, B.-W. Wang and J. Du, *ACS. Appl. Mater. Interfaces.*, 2019, **11**, 11699.

51.   Y. J. Park, B. K. Sharma, S. M. Shinde, M.-S. Kim, B. Jang, J.-H. Kim and J.-H. Ahn, *ACS nano*, 2019, **13**, 3023-3030.

52.   J. Jang, B. Oh, S. Jo, S. Park, H. S. An, S. Lee, W. H. Cheong, S. Yoo and J. U. Park, *Advanced Materials Technologies*, 2019, **4**, 1900082.

53.   R. Yao, Z. Zheng, M. Xiong, X. Zhang, X. Li, H. Ning, Z. Fang, W. Xie, X. Lu and J. Peng, *Applied Physics Letters*, 2018, **112**, 103503.

54.   M. C. McAlpine, H. Ahmad, D. Wang and J. R. Heath, *Nature materials*, 2007, **6**, 379-384.

55.   J. A. Rogers and Y. Huang, *Proceedings of the National Academy of Sciences*, 2009, **106**, 10875-10876.

56.   J. Yoon, A. J. Baca, S.-I. Park, P. Elvikis, J. B. GEDDES III, L. Li, R. H. Kim, J. Xiao, S. Wang and T.-H. Kim, in *Materials for Sustainable Energy: A Collection of Peer-Reviewed Research and Review Articles from Nature Publishing Group*, World Scientific, 2011, pp. 38-46.

57.   A. Javey, S. Nam, R. S. Friedman, H. Yan and C. M. Lieber, *Nano letters*, 2007, **7**, 773-777.

58.   Z. Fan, J. C. Ho, Z. A. Jacobson, R. Yerushalmi, R. L. Alley, H. Razavi and A. Javey, *Nano letters*, 2008, **8**, 20-25.

59.   H. Ning, Y. Zeng, Y. Kuang, Z. Zheng, P. Zhou, R. Yao, H. Zhang, W. Bao, G. Chen and Z. Fang, *ACS Applied Materials & Interfaces*, 2017, **9**, 27792-27800.

60.   Z. Fan, J. C. Ho, Z. A. Jacobson, H. Razavi and A. Javey, *Proceedings of the National Academy of Sciences*, 2008, **105**, 11066-11070.

61.   D. Shahrjerdi and S. W. Bedell, *Nano Lett.*, 2012, **13**, 315-320.

62.   F. Giacomozzi, V. Mulloni, S. Colpo, J. Iannacci, B. Margesin and A. Faes, *Romanian Journal of Information Science and Technology (ROMJIST)*, 2011, **14**, 259-268.

63.   H. Qu, *Micromachines*, 2016, **7**, 14.

64.   J.-H. Seo, K. Zhang, M. Kim, W. Zhou and Z. Ma, *npj Flexible Electronics*, 2017, **1**, 1.

65.   S. Logothetidis, *Materials Science and Engineering: B*, 2008, **152**, 96-104.

66.   B. C.-K. Tee, A. Chortos, A. Berndt, A. K. Nguyen, A. Tom, A. McGuire, Z. C. Lin, K. Tien, W.-G. Bae and H. Wang, *Science*, 2015, **350**, 313-316.

67.   T. W. Kelley, P. F. Baude, C. Gerlach, D. E. Ender, D. Muyres, M. A. Haase, D. E. Vogel and S. D. Theiss, *Chemistry of Materials*, 2004, **16**, 4413-4422.

68.   T. Someya, T. Sekitani, S. Iba, Y. Kato, H. Kawaguchi and T. Sakurai, *Proceedings of the National Academy of Sciences*, 2004, **101**, 9966-9970.

69.   S. Burns, K. Reynolds, W. Reeves, M. Banach, T. Brown, K. Chalmers, N. Cousins, M. Etchells, C. Hayton and K. Jacobs, *Journal of the Society for Information Display*, 2005, **13**, 583-586.

70.   H. Kawaguchi, T. Someya, T. Sekitani and T. Sakurai, *IEEE Journal of Solid-State Circuits*, 2005, **40**, 177-185.

71.   T. Someya, Y. Kato, T. Sekitani, S. Iba, Y. Noguchi, Y. Murase, H. Kawaguchi and T. Sakurai, *Proceedings of the National Academy of Sciences*, 2005, **102**, 12321-12325.

72.   L. Zhou, A. Wanga, S.-C. Wu, J. Sun, S. Park and T. N. Jackson, *Applied Physics Letters*, 2006, **88**, 083502.

73.   M. Mizukami, N. Hirohata, T. Iseki, K. Ohtawara, T. Tada, S. Yagyu, T. Abe, T.

Suzuki, Y. Fujisaki and Y. Inoue, *IEEE Electron Device Lett.*, 2006, **27**, 249-251.

74. Y. Noguchi, T. Sekitani and T. Someya, *Applied physics letters*, 2006, **89**, 253507.

75. Y. Kato, T. Sekitani, M. Takamiya, M. Doi, K. Asaka, T. Sakurai and T. Someya, *IEEE Trans. Electron Devices*, 2007, **54**, 202-209.

76. P. Andersson, R. Forchheimer, P. Tehrani and M. Berggren, *Adv. Funct. Mater.*, 2007, **17**, 3074-3082.

77. I. Yagi, N. Hirai, Y. Miyamoto, M. Noda, A. Imaoka, N. Yoneya, K. Nomoto, J. Kasahara, A. Yumoto and T. Urabe, *Journal of the Society for Information Display*, 2008, **16**, 15-20.

78. T. Sekitani, T. Yokota, U. Zschieschang, H. Klauk, S. Bauer, K. Takeuchi, M. Takamiya, T. Sakurai and T. Someya, *Science*, 2009, **326**, 1516-1519.

79. T. Sekitani, U. Zschieschang, H. Klauk and T. Someya, *Nat. Mater.*, 2010, **9**, 1015.

80. K. Fukuda, T. Sekitani, U. Zschieschang, H. Klauk, K. Kuribara, T. Yokota, T. Sugino, K. Asaka, M. Ikeda and H. Kuwabara, *Adv. Funct. Mater.*, 2011, **21**, 4019-4027.

81. M. Zirkl, A. Sawatdee, U. Helbig, M. Krause, G. Scheipl, E. Kraker, P. A. Ersman, D. Nilsson, D. Platt and P. Bodö, *Adv. Mater.*, 2011, **23**, 2069-2074.

82. T. Yokota, T. Sekitani, T. Tokuhara, N. Take, U. Zschieschang, H. Klauk, K. Takimiya, T.-C. Huang, M. Takamiya and T. Sakurai, *IEEE Trans. Electron Devices*, 2012, **59**, 3434-3441.

83. J. Kawahara, P. Andersson Ersman, D. Nilsson, K. Katoh, Y. Nakata, M. Sandberg, M. Nilsson, G. Gustafsson and M. Berggren, *J. Polym. Sci., Part B: Polym. Phys.*, 2013, **51**, 265-271.

84. M. Kaltenbrunner, T. Sekitani, J. Reeder, T. Yokota, K. Kuribara, T. Tokuhara, M. Drack, R. Schwödiauer, I. Graz and S. Bauer-Gogonea, *Nature*, 2013, **499**, 458.

85. B. Peng, X. Ren, Z. Wang, X. Wang, R. C. Roberts and P. K. Chan, *Scientific reports*, 2014, **4**, 6430.

86. T. Yokota, Y. Inoue, Y. Terakawa, J. Reeder, M. Kaltenbrunner, T. Ware, K. Yang, K. Mabuchi, T. Murakawa and M. Sekino, *Proceedings of the National Academy of Sciences*, 2015, **112**, 14533-14538.

87. X. Ren, K. Pei, B. Peng, Z. Zhang, Z. Wang, X. Wang and P. K. Chan, *Adv. Mater.*, 2016, **28**, 4832-4838.

88. W. Lee, D. Kim, J. Rivnay, N. Matsuhisa, T. Lonjaret, T. Yokota, H. Yawo, M. Sekino, G. G. Malliaras and T. Someya, *Adv. Mater.*, 2016, **28**, 9722-9728.

89. S. Lee, A. Reuveny, J. Reeder, S. Lee, H. Jin, Q. Liu, T. Yokota, T. Sekitani, T. Isoyama and Y. Abe, *Nat. Nanotechnol.*, 2016, **11**, 472.

90. K. Pei, X. Ren, Z. Zhou, Z. Zhang, X. Ji and P. K. L. Chan, *Adv. Mater.*, 2018, **30**, 1706647.

91. M. Kondo, M. Melzer, D. Karnaushenko, T. Uemura, S. Yoshimoto, M. Akiyama, Y. Noda, T. Araki, O. Schmidt and T. Sekitani, *Science advances*, 2020, **6**, eaay6094.

92. G. H. Gelinck, H. E. A. Huitema, E. Van Veenendaal, E. Cantatore, L. Schrijnemakers, J. B. Van Der Putten, T. C. Geuns, M. Beenhakkers, J. B. Giesbers and B.-H. Huisman, *Nat. Mater.*, 2004, **3**, 106.

93. C. Sheraw, L. Zhou, J. Huang, D. Gundlach, T. Jackson, M. Kane, I. Hill, M. Hammond, J. Campi and B. Greening, *Applied physics letters*, 2002, **80**, 1088-1090.

94. Y.-H. Kim, S.-K. Park, D.-G. Moon, W.-K. Kim and J.-I. Han, *Displays*, 2004, **25**, 167-170.

95. P. Mach, S. Rodriguez, R. Nortrup, P. Wiltzius and J. A. Rogers, *Applied Physics Letters*, 2001, **78**, 3592-3594.

96. T. Sekitani, T. Yokota, K. Kuribara, M. Kaltenbrunner, T. Fukushima, Y. Inoue, M. Sekino, T. Isoyama, Y. Abe and H. Onodera, *Nat. Commun.*, 2016, **7**, 11425.

97. M. Choi, B. Jang, W. Lee, S. Lee, T. W. Kim, H. J. Lee, J. H. Kim and J. H. Ahn, *Adv. Funct. Mater.*, 2017, **27**, 1606005.

98. T. Sekitani, Y. Noguchi, K. Hata, T. Fukushima, T. Aida and T. Someya, *Science*, 2008, **321**, 1468-1472.

99. T. Sekitani, H. Nakajima, H. Maeda, T. Fukushima, T. Aida, K. Hata and T. Someya, *Nat. Mater.*, 2009, **8**, 494.

100. S. Y. Hong, Y. H. Lee, H. Park, S. W. Jin, Y. R. Jeong, J. Yun, I. You, G. Zi and J. S. Ha, *Adv. Mater.*, 2016, **28**, 930-935.

101. C. W. Park, J. B. Koo, C.-S. Hwang, H. Park, S. G. Im and S.-Y. Lee, *Applied Physics Express*, 2018, **11**, 126501.

102. D. S. Kim, H. Park, S. Y. Hong, J. Yun, G. Lee, J. H. Lee, L. Sun, G. Zi and J. S. Ha, *Appl. Surf. Sci.*, 2019, **471**, 300-308.

103. K. Sim, Z. Rao, H.-J. Kim, A. Thukral, H. Shim and C. Yu, *Science advances*, 2019, **5**, eaav5749.

104. D. S. Gray, J. Tien and C. S. Chen, *Adv. Mater.*, 2004, **16**, 393-397.

105. Q. Gao, H. Li, J. Zhang, Z. Xie, J. Zhang and L. Wang, *Scientific reports*, 2019, **9**, 5908.

106. Y. Yang, N. Sun, Z. Wen, P. Cheng, H. Zheng, H. Shao, Y. Xia, C. Chen, H. Lan and X. Xie, *ACS nano*, 2018, **12**, 2027-2034.

107. J. Y. Oh, S. Rondeau-Gagné, Y.-C. Chiu, A. Chortos, F. Lissel, G.-J. N. Wang, B. C. Schroeder, T. Kurosawa, J. Lopez and T. Katsumata, *Nature*, 2016, **539**, 411.

108. H.-J. Kim, K. Sim, A. Thukral and C. Yu, *Sci. Adv.*, 2017, **3**, e1701114.

109. H. Shim, K. Sim, F. Ershad, P. Yang, A. Thukral, Z. Rao, H.-J. Kim, Y. Liu, X. Wang and G. Gu, *Science advances*, 2019, **5**, eaax4961.

110. J. Xu, S. Wang, G.-J. N. Wang, C. Zhu, S. Luo, L. Jin, X. Gu, S. Chen, V. R. Feig and J. W. To, *Science*, 2017, **355**, 59-64.

111. A. F. Paterson, S. Singh, K. J. Fallon, T. Hodsden, Y. Han, B. C. Schroeder, H. Bronstein, M. Heeney, I. McCulloch and T. D. Anthopoulos, *Advanced Materials*, 2018, **30**, 1801079.

112. X. Jia, C. Fuentes-Hernandez, C.-Y. Wang, Y. Park and B. Kippelen, *Science advances*, 2018, **4**, eaao1705.

113. M. J. Kim, M. Lee, H. Min, S. Kim, J. Yang, H. Kweon, W. Lee, D. H. Kim, J.-H. Choi and D. Y. Ryu, *Nature communications*, 2020, **11**, 1-11.

114. E. K. Lee, C. H. Park, J. Lee, H. R. Lee, C. Yang and J. H. Oh, *Advanced Materials*, 2017, **29**, 1605282.

115. J. A. DeFranco, B. S. Schmidt, M. Lipson and G. G. Malliaras, *Organic Electronics*, 2006, **7**, 22-28.

116. H. Minemawari, T. Yamada, H. Matsui, J. y. Tsutsumi, S. Haas, R. Chiba, R. Kumai and T. Hasegawa, *Nature*, 2011, **475**, 364-367.

117. H. Sirringhaus, T. Kawase, R. Friend, T. Shimoda, M. Inbasekaran, W. Wu and E. Woo, *Science*, 2000, **290**, 2123-2126.

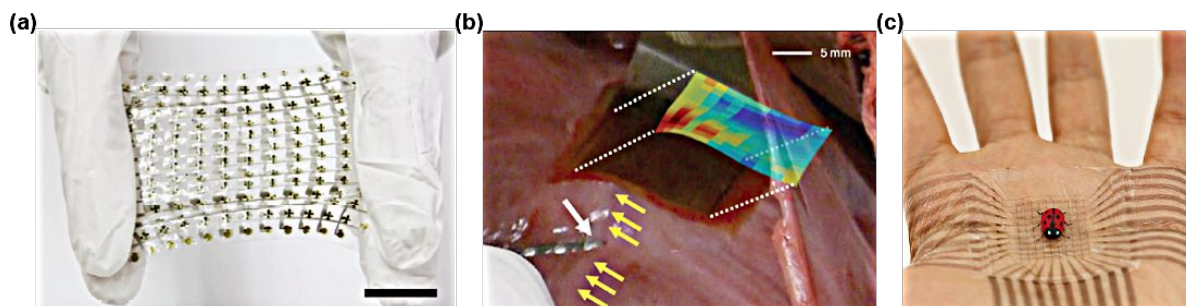118. Z. Bao and X. Chen, *Advanced Materials*, 2016, **28**, 4177-4179.

**Figure 1** (a) A stretchable active matrix. Scale bar: 20 mm. Reproduced with permission from ref. 12. Copyright 2015, Springer Nature. (b) A flexible electrophysiology mapping device on the porcine heart. Reproduced with permission from ref. 13. Copyright 2010, American Association for the Advancement of Science. (c) A stretchable active matrix conforms to a human palm, enabling accurate sensing of the position of a synthetic ladybug with six conductive legs. Reproduced with permission from ref. 14. Copyright 2018, Springer Nature.
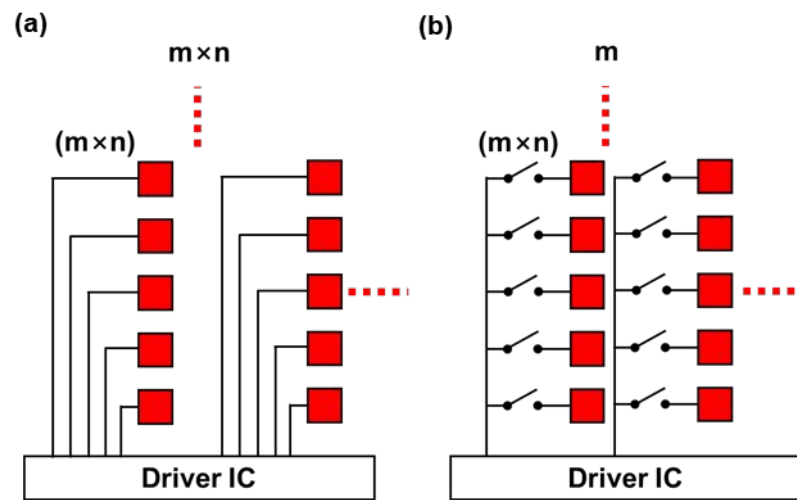
**Figure 2** Schematic diagram of (a) direct addressing and (b) matrix addressing.
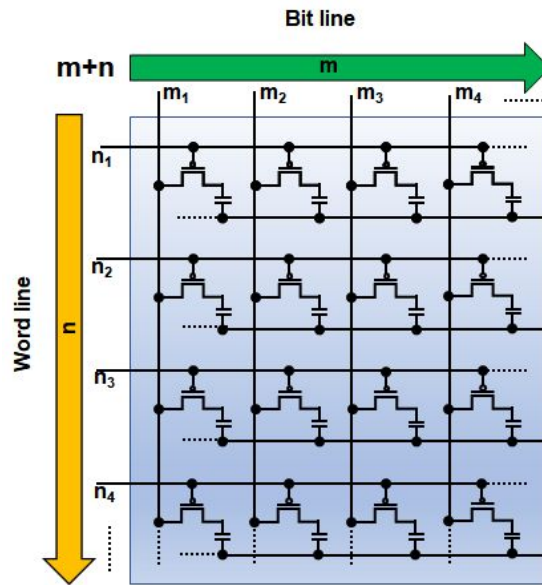
**Figure 3** Typical transistor array for active matrix addressing.
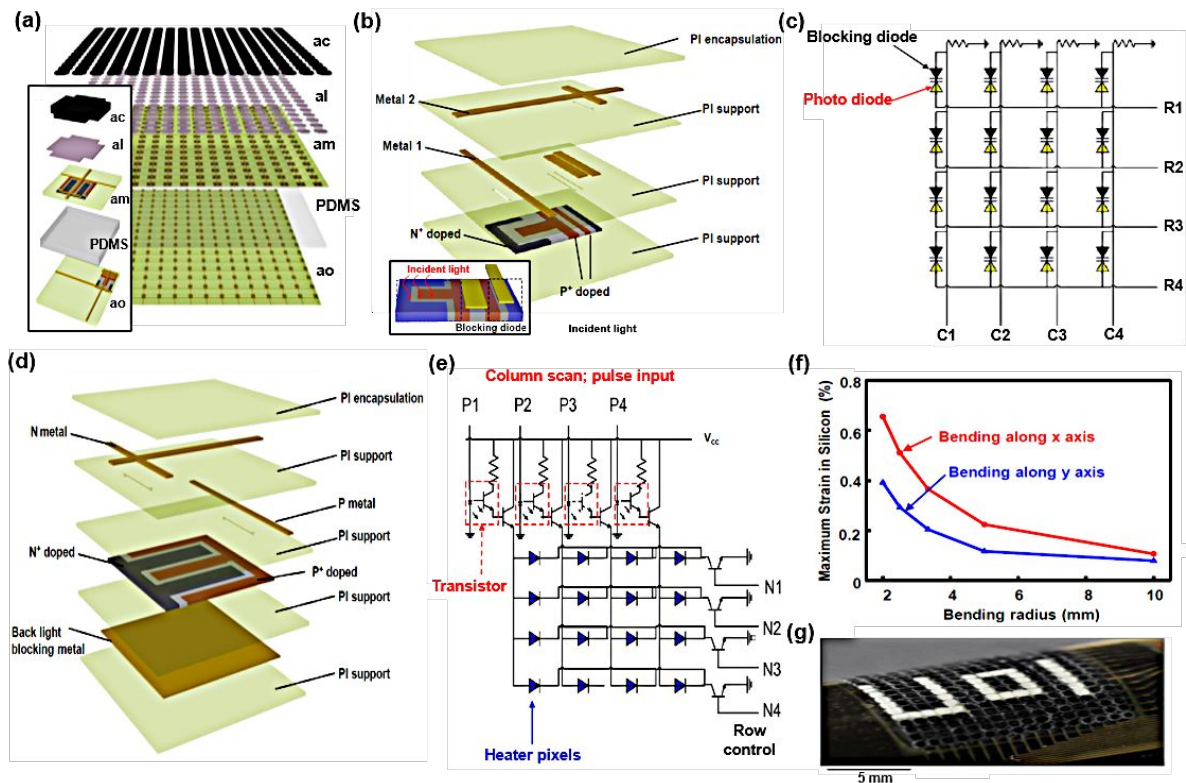
**Figure 4** (a) Exploded view of illustration of a 16×16 array of interconnected unit cells in a full, adaptive camouflage skin. (b) The schematic exploded view of sensing part includes a photodiode and a multiplexing (blocking) diode connected in a back-to-back fashion. (c) A circuit diagram for sensing part. (d) The schematic exploded view of heating part with multiplexed addressing. (e) A circuit diagram for heating part. (f) Maximum strain in silicon depending on the bending radius. (g) Image of a device in operation while bent, while showing the text pattern "U o I". Reproduced with permission from ref. 5. Copyright 2014, National Academy of Sciences.
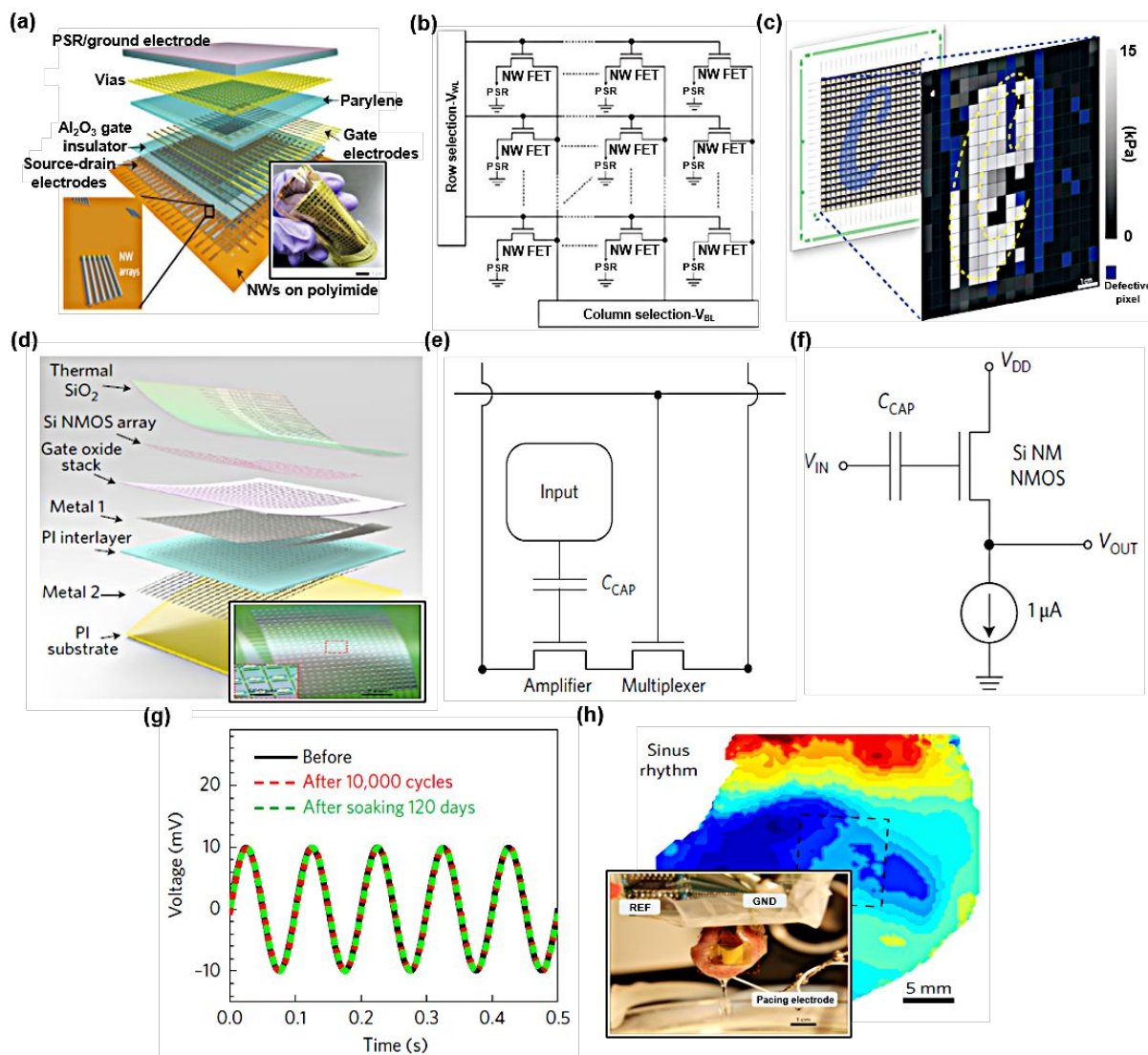
**Figure 5** (a) An exploded view of a flexible active matrix based e-skin. (b) Optical microscope image of a single sensor pixel in the array (left) and circuitry of active matrix (right). (c) Design layout of the active matrix (left) and the corresponding mapping results from pixel signals (right). Reproduced with permission from ref. 37. Copyright 2010, Springer Nature. (d) An exploded view of a completed capacitively coupled flexible sensing system. (e) A circuit diagram for each sensor. (f) A circuit of a common drain amplifier (source follower). (g) The response of a representative node to a sine wave input at 10 Hz before and after 10000 cycles of bending and after saline immersion (for 120 days). (h) Electrical mapping results from a rabbit heart during the sinus rhythm. Reproduced with permission from ref. 46. Copyright 2017,
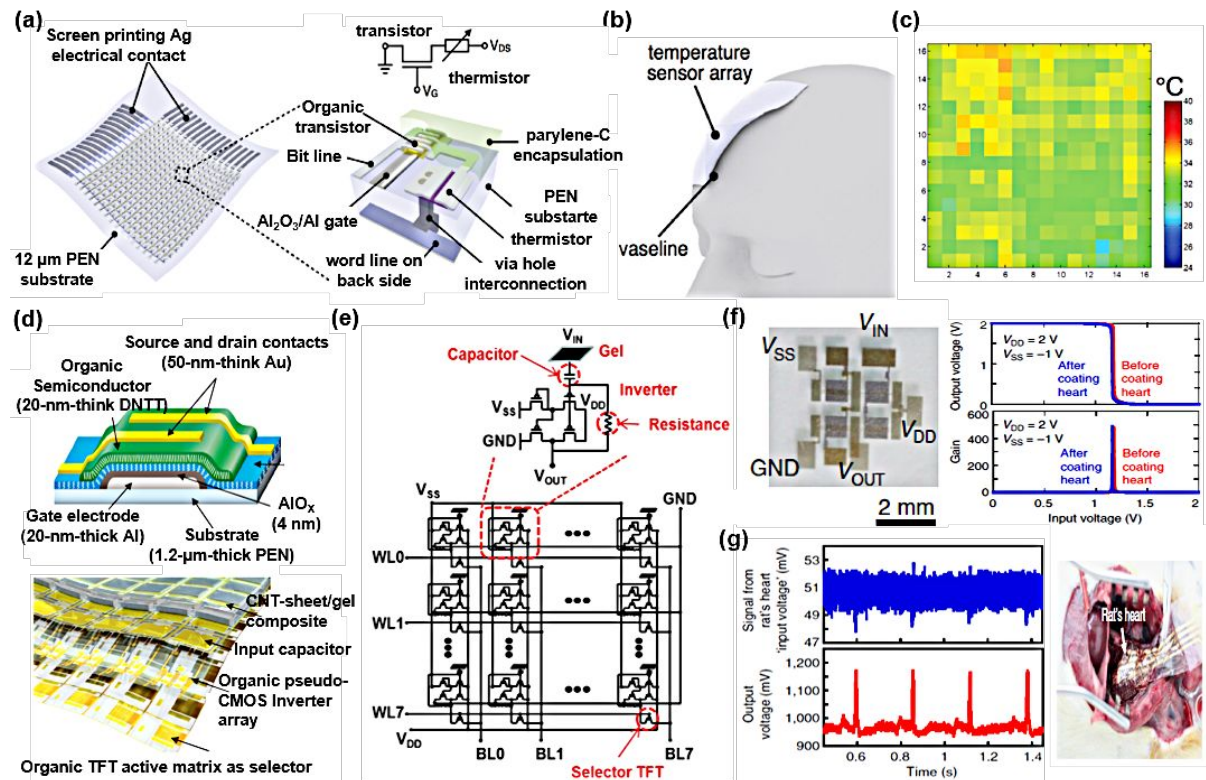
Springer Nature.



**Figure 6** (a) The schematic structure of the 16 × 16 temperature sensor array and schematic diagram of a single temperature sensor. (b) Schematic cross-sectional image of the experimental setup. (c) Temperature distribution measured from active matrix based temperature sensor array on the forehead. Reproduced with permission from ref. 87. Copyright 2016, Wiley-VCH. (d) A schematic cross-sectional diagram of the transistor (top) and a schematic illustration of the flexible active matrix based amplifier array (bottom). (e) A circuit diagram of the flexible active matrix amplifier array. (f) The photograph (left) and voltage transfer curve (right) of the organic pseudo-CMOS inverter. (g) ECG before and after amplifying (left) and the photograph of the ultra-flexible active matrix applied to the rat's heart (right). Reproduced with permission from ref. 96. Copyright 2016, Springer Nature.
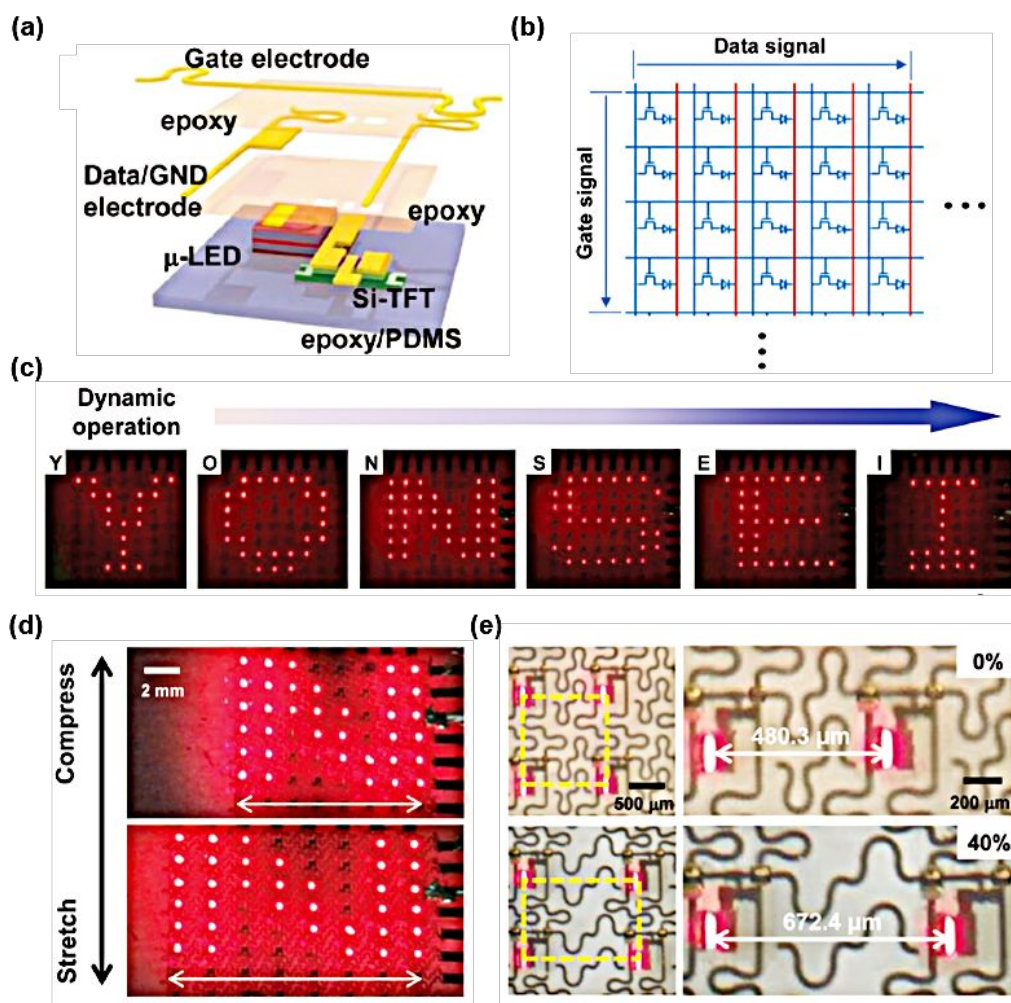
**Figure 7** (a) Schematic of the single pixel structure. (b) Equivalent circuit diagram of the active matrix display. (c) Dynamic operation of the active matrix display on a PDMS substrate. (d) A stretchable active matrix display, showing emission characteristics under mechanical strain. (e) The magnified image of the stretched active matrix display under mechanical strain. Reproduced with permission from ref. 97. Copyright 2017, Wiley-VCH.
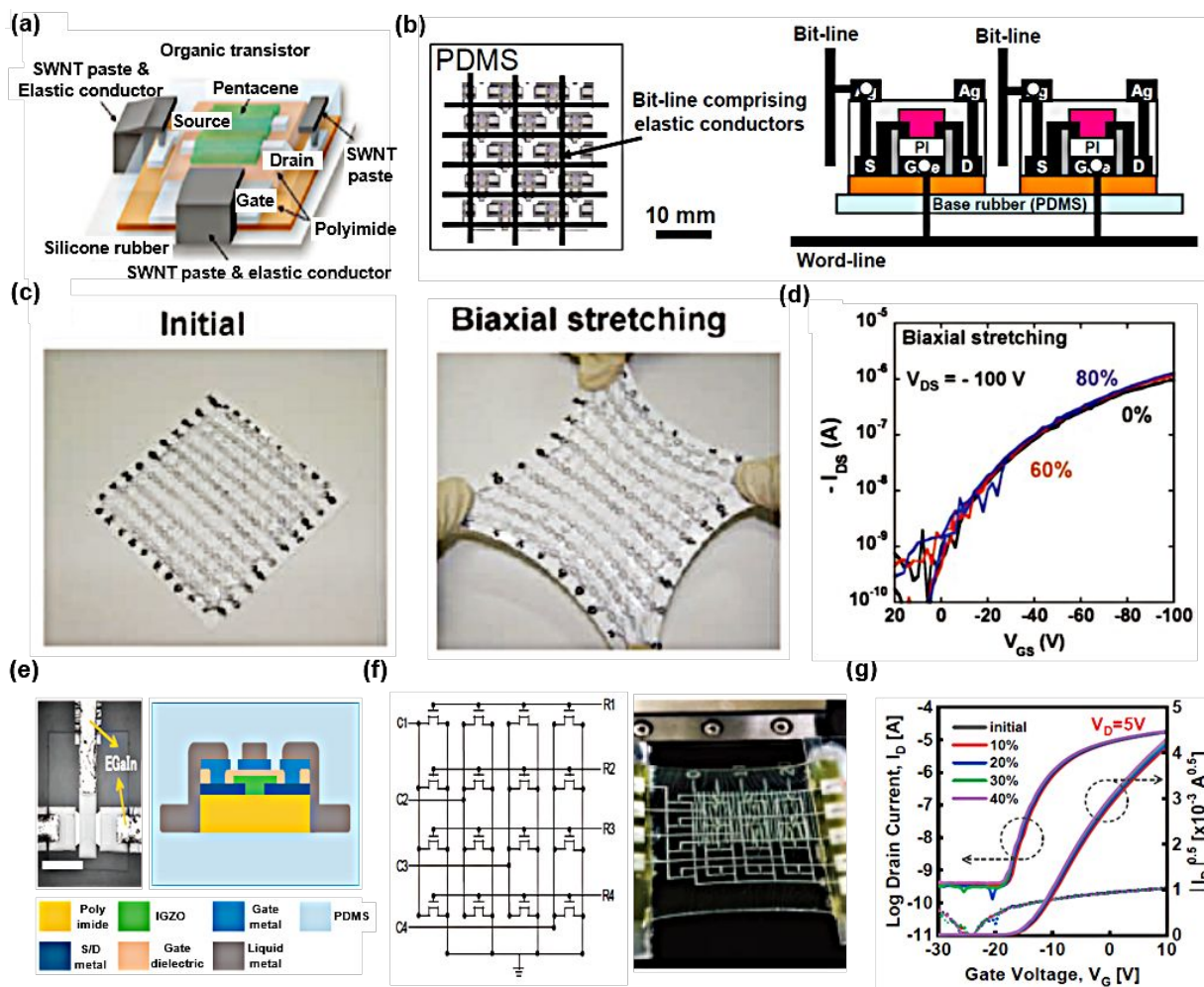
**Figure 8** (a) The structure of the organic transistor. (b) Top (left) and cross-sectional view (right) of a stretchable active matrix. (c) Images of the stretchable active matrix before stretching and under biaxial stretching. (d) Transfer curve of the transistor under mechanical strain. Reproduced with permission from ref. 98. Copyright 2008, American Association for the Advancement of Science. (e) Optical microscope image (left) and schematic cross-sectional view of a transistor (right). (f) The circuitry and photograph of a deformed 4 × 4 oxide transistor based active matrix. (g) The transfer curve of the oxide transistor under mechanical strain. Reproduced with permission from ref. 101. Copyright 2018, IOPscience.
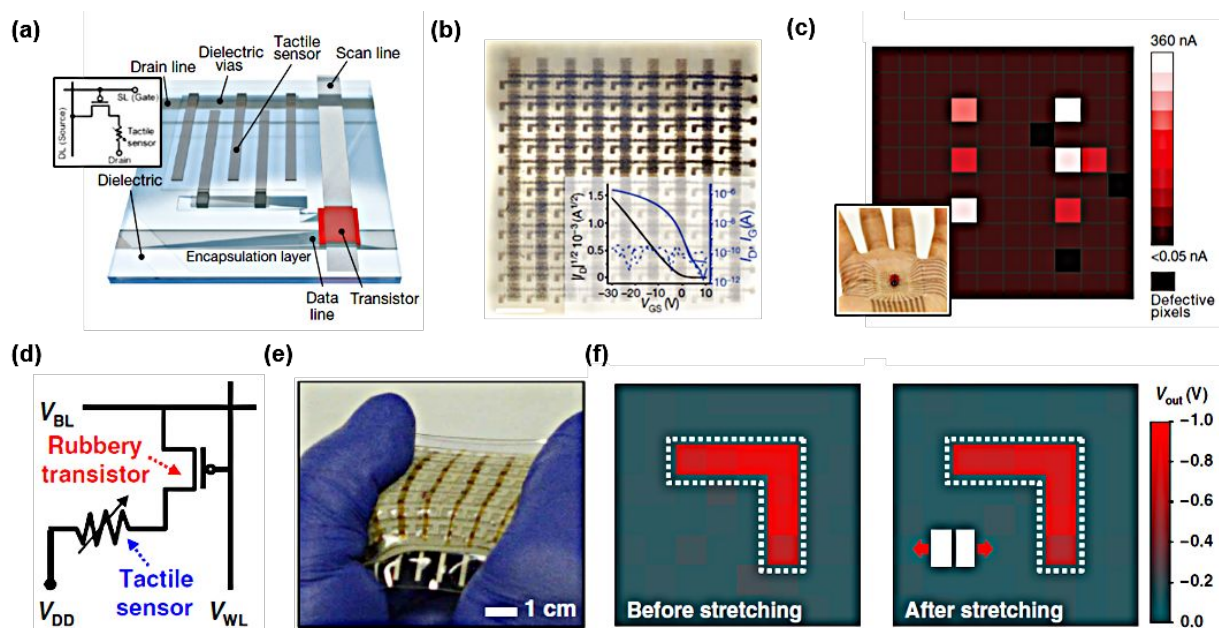
**Figure 9** (a) Schematic of the single pixel structure from the stretchable active matrix. (b) The photograph of the stretchable active matrix (left) and individual transfer curve of the transistor (right) (c) Current mapping depending on the position of the ladybug. Reproduced with permission from ref. 14. Copyright 2018, Springer Nature. (d) A circuit for a single pixel. (e) The deformed fully rubbery active matrix under stretching. (f) Voltage mapping results before and after mechanical strain of 30 % along the channel length direction. Reproduced with permission from ref. 103. Copyright 2019, American Association for the Advancement of Science.

| Deformation mode | Substrate | Semiconductor | Bending radius (mm)/ Strain range (%) | Applications | Ref. # |
|---|---|---|---|---|---|
| **Flexible** | PI | p, n-doped Si | 2 mm | Camouflage system | 5 |
| | PI | Ge/Si core/shell nanowire | 2.5 mm | Pressure sensor | 37 |
| | PI | CNT | 4 mm | Display | 40 |
| | PI | p, n-doped Si | 5 mm | Bioelectronics | 46 |
| | PET | MoS$_2$ | 0.7 mm | Display | 48 |
| | PI | DNTT | 0.7 mm | Temperature sensor | 86 |
| | PEN | DNTT | 3.2 mm | Temperature sensor | 87 |
| | Parylene | DNTT | 2 mm | Amplifier | 91 |
| | PEN | DNTT | 0.05 mm | Amplifier | 96 |
| **Stretchable** | Epoxy/PDMS | p, n-doped Si | 15 mm / 40 % | Display | 97 |
| | PI/PDMS | Pentacene | 120% | OTFT array | 98 |
| | PET/Ecoflex | SWCNT | 14 mm / 30 % | Temperature sensor | 100 |
| | PI/PDMS | IGZO | 40 % | TFT array | 101 |
| | SEBS | 29-DPP-SVS/SEBS | 100% | Tactile sensor | 14 |
| | PDMS | P3HT NFs/PDMS | 50% | Tactile sensor | 103 |
| | SEBS | DPP-polymer | 25~100% | OTFT array | 107 |

**Table 1** Summary of the materials and applications of soft active matrix devices.

Journal of Materials Chemistry C

**Table of Content Entry**
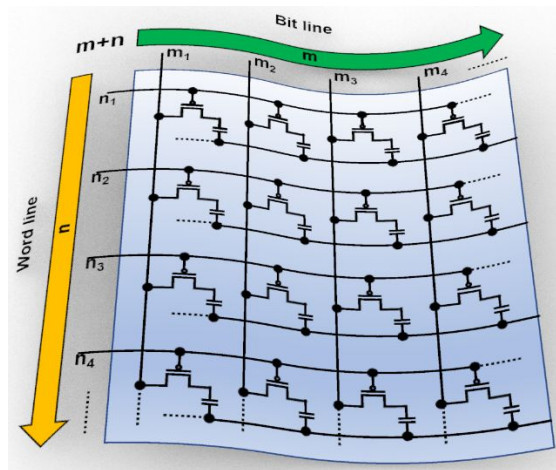


The review paper provides an overview of the recent development in flexible and stretchable active matrix electronics for various applications.